International Journal of Thermophysics, Vol. 28, No. 1, February 2007 (© 2007)
DOI: 10.1007/s10765-007-0157-3

"Thermal Mirror" Method for Measuring Physical Properties of Multilayered Coatings

T. Elperin[1,2] and G. Rudin[1]

Received: March 29, 2006

In this study theoretical principles underlying the photothermal displacement ("thermal mirror") method for measuring physical properties of opaque multilayered and functionally graded coatings with low thermal conductivity are analyzed. In this method, the specimen is locally heated by a power laser beam, and a two-dimensional transient temperature field is formed in a specimen. The physical basis for the photothermal displacement method is the non-stationary buckling and displacement of an irradiated surface due to a non-uniform thermal expansion. The surface is monitored by a low-power probe beam of a second laser, which is reflected from the specimen, i.e., the system operates as a convex "thermal mirror." The photoinduced displacement varies with time, and the probe beam is reflected at a different angle depending on the slope of the displacement. The deflection angle is measured as a function of time by a position sensor, and the results of these measurements are compared with the theoretical dependence of the deflection angle on time and physical properties of a coating. This dependence was determined analytically from the solution of the two-dimensional thermal elasticity problem. It is shown that for the specimen composed of a substrate and a coating it is feasible to determine the properties of the coating, e.g., the thermal diffusivity and coefficient of linear thermal expansion provided that the analogous properties of the substrate are previously measured or otherwise known.

KEY WORDS: laser heating; multilayer coating; surface displacement; thermal elasticity.

[1] Department of Mechanical Engineering, Pearlstone Center for Aeronautical Engineering Studies, Ben-Gurion University of the Negev, P. O. Box 653, Beer-Sheva 84105, Israel.
[2] To whom correspondence should be addressed. E-mail: elperin@bgu.ac.il

1. INTRODUCTION

The evaluation of physical properties of solids, surfaces, thin coatings, and films has become an important problem due to wide scientific and technological applications (optics, electronics, design of advanced materials used for manufacturing of thermal barriers and impact-resistant coatings, etc.). There are a number of photothermal techniques for the measurement of physical properties of materials, e.g., photothermal displacement spectroscopy [1], photoacoustic spectroscopy, photothermal radiometry [2–5], and the "mirage effect" [2,6]. These contact-free highly sensitive methods successfully overcome many difficulties inherent in the traditional contact methods. All photothermal methods are based on irradiation of the investigated specimen by coherent or incoherent electromagnetic radiation that is absorbed at the surface or in a sub-surface region of a sample and results in heating of the material (photothermal heating effect). Heating results in a number of physical changes in the sample, such as thermal expansion, thermal stresses, infrared emission, buckling of the surface, etc. These changes can be detected by one of the following three detection schemes, namely, acoustic, optical, or thermal (a review of these methods is presented in Ref. 2). A theoretical investigation of the photothermal method is required for determining the dependence of the registered signal on the surface and bulk physical properties of the sample. Comparing the registered information in the experiment signal with the theoretically predicted results, one can determine physical properties of a sample.

The subject of this study is the photothermal displacement ("thermal mirror") method that is based on irradiation of the investigated sample by a laser pulse. The absorbed electromagnetic radiation causes a local increase of temperature (in the range from a few kelvin for measuring physical properties to several hundred kelvin for reliability testing of coatings), non-uniform thermal expansion, and buckling of the illuminated surface. The probe beam of a second laser that does not heat the specimen is directed at the buckling surface. Due to non-stationary buckling of the surface, the probe beam reflection angle varies, i.e., a coating operates as a convex "thermal mirror" (see Fig. 1). Clearly, the reflection angle depends on the temperature and strain fields and, consequently, upon the physical properties of a specimen. The measured magnitudes of the deflection angle are compared with theoretical results in order to determine the physical properties.

Usually, the photothermal displacement is a small perturbation of the specimen surface. For the case when the temperature rise is of the order of 1–10 K, the maximum value of the slope of a coating surface is of the order of 10^{-5}, and it can be registered by commercially available devices.

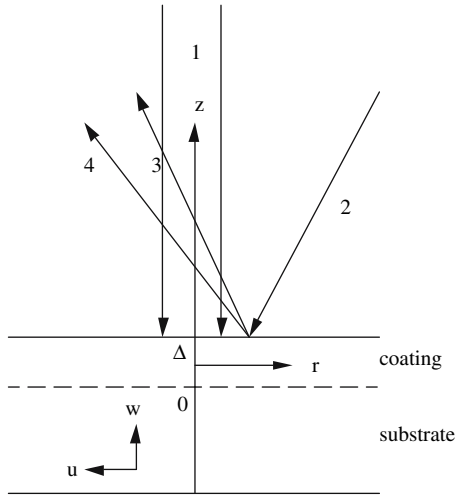

Fig. 1. Schematic diagram of the photothermal displacement method: (1) power laser beam; (2) probe laser beam; (3, 4) reflected probe beam before and after irradiation of a coating by a power beam.

Thus, e.g. [1] measured a slope of the order of 10^{-8}. This method can also be employed for reliability testing of coatings in both passive and active modes [7]. In this case, the maximum temperature rise and thermal stresses in a specimen are of the order of 100 K and 100 MPa, respectively. When the method is used for reliability testing in a passive mode for detecting a failure of a coating (e.g., loss of the bond integrity), the temperature elevation is of the order of several tens of kelvin.

Due to non-uniform heating, a coating is subjected to thermal deformation that causes significant buckling of the surface at the location of the defect whereby a gap between a coating and a substrate is formed. The rate of buckling of a disbonded coating differs from that for the case of a perfect coating. Therefore, the analysis of the temporal relaxation of a slope of the specimen surface allows detection of subsurface defects [2]. In order to employ the photothermal method for reliability testing in an active mode, it is necessary to increase the laser pulse energy, and, hence, the thermal stresses in a coating until damage occurs. This allows determination of the threshold value of the thermal load that results in irreversible damage of a coating.

In this paper we present a methodology and theory of the photothermal displacement method for measuring physical properties of multilayered

and functionally graded coatings. Application of the photothermal displacement method for functionally graded materials (FGMs) attracted considerable interest in recent years [8,9]. These advanced composite materials are developed using coatings with a thickness of the order of 10–100 μm for metal elements, which are subjected to thermal loads in a high-temperature environment. The typical FGM coating is composed primarily of technical ceramics on the front side of the element, primarily of metal on the rear side, and an intermediate layer with the composition changing continuously from ceramic to metal. The FGM coating is designed so that it reduces significantly the thermal stresses in a protected metallic element.

In order to evaluate the behavior of a coating under an intensive thermal load, it is necessary to determine the physical properties of an FGM. The continuous variation of the composition across a coating changes the physical properties of the FGM in the direction normal to the surface and, therefore, the traditional methods used to measure physical properties of solids cannot be applied [8]. Moreover, the physical properties of a coating depend on the manufacturing process used for its production, e.g., thermal spray deposition, plasma spray forming, laser cladding with direct powder injection, etc. Usually the FGM coating is prepared by the "layer by layer" method with different volume content of ceramics, thus producing the desired through-thickness gradient of the thermal and mechanical properties of a coating. The photothermal displacement method, as applied to FGMs, involves measuring a property of a coating after deposition of each individual thin layer, e.g., layer by layer, until completion of the formation of a coating. In this study the problems of thermal elasticity for a multilayer coating and a functionally graded coating are investigated within the framework of a unified approach because the FGM can be represented as a multilayer assembly with infinitesimally small thicknesses of the individual layers provided that the number of layers tends to infinity.

We investigated the photothermal displacement method for measuring the properties of coatings that have a thermal conductivity low in comparison with that of the substrate and that have found wide applications as thermal barriers, and tribological or impact-resistant coatings. The main goals of this study are as follows:

(a) Development of the analytical procedure for the solution of the two-dimensional transient thermal elasticity problem in a multilayer coating-substrate assembly which can be further used for FGMs
(b) Derivation of expressions for the surface displacement and the probe beam deflection angle (the main measured parameters) in a convenient form for comparing the experimental results with the theoretical

values. For the case of a single-layer coating, these expressions are compared with the exact solution of the problem. The surface displacement and deflection angle depend on operating parameters of the photothermal method (laser power, radius of laser beam, distance between the power beam and the probe beam axes) and the physical properties of a coating.

(c) Development of an algorithm that allows determination of the physical properties of a coating by comparing the measured result of the deflection angle with the theoretical value given by the obtained analytical solution.

The theoretical foundation of the photothermal displacement method for measuring physical properties is based on a solution of the non-stationary thermal elasticity problem, determining the photoinduced displacement and slope of the coating surface.

2. SOLUTION OF THE THERMAL ELASTICITY PROBLEM

Consider a thermal elasticity problem for a thin n-layer coating deposited on a substrate and heated by a power laser beam incident at $z=\Delta$ in a direction normal to the surface (Fig. 1). The temperature rise in a specimen is governed by a non-stationary two-dimensional heat conduction equation with the appropriate initial and boundary conditions ($i=1,\ldots,n$ is the number of a layer in a coating, $i=0$ for a substrate):

$$c_i \frac{\partial T_i}{\partial t} = \lambda_i \left[\frac{1}{r} \frac{\partial}{\partial r} \left(r \frac{\partial T_i}{\partial r} \right) + \frac{\partial^2 T_i}{\partial z^2} \right], \tag{1}$$

$$T_i|_{t=0} = \left. \frac{\partial T_i}{\partial z} \right|_{r=\infty} = \left. \frac{\partial T_0}{\partial z} \right|_{z=-\infty} = 0, \quad \lambda_n \left. \frac{\partial T_n}{\partial z} \right|_{z=\Delta} = I_0 \exp\left(-\frac{r^2}{r_0^2} \right) H(\tau_0 - t). \tag{2}$$

We assume that a substrate can be represented as a semi-infinite body since the Fourier number is small, i.e., $Fo = k_0 t / d^2 \ll 1$. The external layer is assumed optically opaque since the absorption length is small in comparison with its thickness.

The continuity of temperature and the thermal flux at the boundaries between adjacent layers yield

$$T_{i-1} = T_i, \quad \lambda_{i-1} \frac{\partial T_{i-1}}{\partial z} = \lambda_i \frac{\partial T_i}{\partial z} \quad \text{at the interface } z = \sum_{k=1}^{i} \Delta_k. \tag{3}$$

Next, we determine the strain and stress distributions in a multilayer coating-substrate assembly caused by the non-uniform temperature field. The radial, u_i, and axial, w_i, displacements are governed by a quasi-stationary Navier equation [10]:

$$\frac{1}{r}\frac{\partial}{\partial r}\left(r\frac{\partial u_i}{\partial r}\right)+\frac{\partial^2 u_i}{\partial z^2}-\frac{u_i}{r^2}+\frac{1}{1-2\nu_i}\frac{\partial e_i}{\partial r}=2\alpha_i\frac{1+\nu_i}{1-2\nu_i}\frac{\partial T_i}{\partial r},$$
$$\frac{1}{r}\frac{\partial}{\partial r}\left(r\frac{\partial w_i}{\partial r}\right)+\frac{\partial^2 w_i}{\partial z^2}+\frac{1}{1-2\nu_i}\frac{\partial e_i}{\partial z}=2\alpha_i\frac{1+\nu_i}{1-2\nu_i}\frac{\partial T_i}{\partial z},\quad i=0,\ldots,n, \tag{4}$$

where $e_i=\frac{\partial u_i}{\partial r}+\frac{u_i}{r}+\frac{\partial w_i}{\partial z}$ is the volume expansion of a layer i. The elastic stresses are determined from the Duhamel–Neumann relations;

$$(\sigma_{rz})_i = G_i\left(\frac{\partial u_i}{\partial z}+\frac{\partial w_i}{\partial r}\right),$$
$$(\sigma_{zz})_i = 2G_i\left[\frac{\partial w_i}{\partial z}+\frac{\nu_i}{1-2\nu_i}e_i-\alpha_i\frac{1+\nu_i}{1-2\nu_i}T_i\right]. \tag{5}$$

The boundary and continuity conditions for the thermal stresses and displacements yield

$$(\sigma_{rz})_n = (\sigma_{zz})_n=0 \text{ at } z=\Delta, (\sigma_{rz})_{i-1}=(\sigma_{rz})_i,$$
$$(\sigma_{zz})_{i-1} = (\sigma_{zz})_i, u_{i-1}=u_i, \tag{6}$$
$$w_{i-1}=w_i \quad \text{at the interface } z=\sum_{k=1}^{i}\Delta_k.$$

Applying the Laplace–Hankel transform to Eq. (1) and the initial and boundary conditions in Eqs. (2) and (3), we obtain

$$\frac{\partial^2\bar{\theta}_i}{\partial z^2}=\left(\frac{s}{k_i}+p^2\right)\bar{\theta}_i,\quad \bar{\theta}_i\big|_{t=0}=\left.\frac{\partial\bar{\theta}_i}{\partial z}\right|_{r=\infty}=\left.\frac{\partial\bar{\theta}_0}{\partial z}\right|_{z=-\infty}=0,$$
$$\lambda_n\left.\frac{\partial\bar{\theta}_n}{\partial z}\right|_{z=\Delta}=\frac{I_0 r_0^2}{2}\exp\left(-\frac{p^2 r_0^2}{4}\right)\frac{1-\exp(-\tau_0 s)}{s}, \tag{7}$$

$$\bar{\theta}_{i-1}=\bar{\theta}_i,\quad \lambda_{i-1}\frac{\partial\bar{\theta}_{i-1}}{\partial z}=\lambda_i\frac{\partial\bar{\theta}_i}{\partial z}, \tag{8}$$

where

$$\bar{\theta}_i(s,p,z)=\int_0^\infty\int_0^\infty T_i(t,r,z)\exp(-st)\,r J_0(pr)\,\mathrm{d}t\,\mathrm{d}r. \tag{9}$$

Table I. Thermophysical and Mechanical Properties of Materials

Material	$\lambda(W\cdot m^{-1}\cdot K^{-1})$	$c(J\cdot m^{-3}\cdot K^{-1})$	$\alpha(K^{-1})$	G (GPa)
Ni	69	4.6×10^{6}	14×10^{-6}	80
ZrO_2	2.0	5.0×10^{6}	10×10^{-6}	73
$Ni+ZrO_2$ (40%)	4.8	4.8×10^{6}	12.4×10^{-6}	75.3
$Ni+ZrO_2$ (80%)	2.5	5.0×10^{6}	9.7×10^{-6}	55.4

In order to calculate w in Eq. (4), it is necessary to determine the Hankel transform of the two-dimensional temperature field $\theta_i(p,z)$ in a coating. An analytical solution of the two-dimensional heat conduction problem in a multilayer assembly does not exist. For the particular case of a small Fourier number, $Fo=\left(k_n/\Delta_n^2+k_{n-1}/\Delta_{n-1}^2\right)t\ll1$, the temperature field is localized in the layers n and $(n-1)$ of a coating (this assumption can be easily fulfilled under the experimental conditions because the thermal diffusivities, k_n and k_{n-1}, are small (see Table I).

The general solution of Eq. (7) reads

$$\bar{\theta}_{n-1}=A_{n-1}\exp\left(\gamma_{n-1}z\right),\quad \bar{\theta}_n=A_n\exp\left(\gamma_n z\right)+B_n\exp\left(-\gamma_n z\right), \tag{10}$$

where $\gamma_i=\sqrt{\frac{s}{k_i}+p^2}$, A_{n-1}, A_n, and B_n are the integration constants that are determined from the continuity and boundary conditions in Eqs. (7) and (8). Substituting Eq. (10) into Eq. (7) and after some algebra, we arrive at the expressions for the Laplace–Hankel transform of temperature distributions:

$$\begin{aligned}\bar{\theta}_{n-1}&=\frac{I_0r_0^2}{\lambda_n\gamma_n}\frac{a_n}{a_n+1}\frac{1}{b_n}\exp\left(-\frac{p^2r_0^2}{4}\right)\frac{1-\exp\left(-\tau_0 s\right)}{s}\exp\left(\gamma_{n-1}z'-\gamma_n\Delta_n\right),\\ \bar{\theta}_n&=\frac{I_0r_0^2}{2\lambda_n\gamma_n}\frac{1}{b_n}\exp\left(-\frac{p^2r_0^2}{4}\right)\frac{1-\exp\left(-\tau_0 s\right)}{s}\left\{\exp\left[-\gamma_n\left(\Delta_n-z'\right)\right]+\frac{a_n-1}{a_n+1}\right.\\ &\left.\times\exp\left[-\gamma_n\left(\Delta_n+z'\right)\right]\right\},\quad \bar{\theta}_0=\bar{\theta}_1=\ldots=\bar{\theta}_{n-2}=0,\end{aligned} \tag{11}$$

where

$$a_n=\frac{\lambda_n\gamma_n}{\lambda_{n-1}\gamma_{n-1}},\quad b_n=1-\frac{a_n-1}{a_n+1}\exp\left(-2\gamma_n\Delta_n\right),\quad z'=z-\sum_{m=0}^{n-1}\Delta_m. \tag{12}$$

Since under the experimental conditions, the Fourier number $Fo \ll 1$, i.e., $|s| \gg k_n / r_0^2$, Eq. (12) can be approximated as

$$a_n \approx \frac{\lambda_n \sqrt{k_{n-1}}}{\lambda_{n-1} \sqrt{k_n}}, \quad \frac{1}{b_n} = \sum_{m=0}^{\infty} \left(\frac{a_n - 1}{a_n + 1} \right)^m \exp\left(-2m\gamma_n \Delta_n\right). \tag{13}$$

Substituting Eq. (13) into Eq. (11) and using the convolution theorem and the tables of the inverse Laplace transform, we determine the Hankel transforms of temperature distributions for $t \gg \tau_0$:

$$\begin{aligned}
&\theta_n(t, p, z) \\
&= \frac{E_0 \sqrt{k_n}}{2\pi^{3/2} \lambda_n \sqrt{t}} \exp\left[-p^2 \left(0.25 r_0^2 + k_n t\right)\right] \sum_{m=0}^{\infty} \left(\frac{a_n - 1}{a_n + 1} \right)^m \\
&\times \left\{ \exp\left[-\frac{\left(2m\Delta_n + \Delta_n - z'\right)^2}{4k_n t} \right] + \frac{a_n - 1}{a_n + 1} \exp\left[-\frac{\left(2m\Delta_n + \Delta_n + z'\right)^2}{4k_n t} \right] \right\}, \\
&\theta_{n-1}(t, p, z) \\
&= \frac{E_0}{2\pi^2 \lambda_n} \frac{a_n |z'|}{a_n + 1} \sqrt{\frac{k_n}{k_{n-1}}} \exp\left[-p^2 \left(0.25 r_0^2 + k_n t\right)\right] \int_0^t \frac{1}{\sqrt{t_0^3 (t - t_0)}} \\
&\times \exp\left[-\left(z'\right)^2 / 4k_{n-1} t_0 \right] \exp\left[-p^2 (k_{n-1} - k_n) t_0 \right] \sum_{m=0}^{\infty} \left(\frac{a_n - 1}{a_n + 1} \right)^{\mathrm{m}} \\
&\exp\left[-\frac{(2m+1)^2 \Delta_n^2}{4k_n (t - t_0)} \right] \mathrm{d}t_0, \quad z' = z - \sum_{m=0}^{n-1} \Delta_m, \; a_n = \frac{\lambda_n \sqrt{k_{n-1}}}{\lambda_{n-1} \sqrt{k_n}}, \\
&\theta_0 = \theta_1 = \cdots = \theta_{n-2} = 0.
\end{aligned} \tag{14}$$

Formulas for the Hankel transforms of the displacements u_i, w_i in the radial and axial directions, respectively, are expressed as

$$\varphi_i(t, p, z) = \int_0^{\infty} u_i(t, r, z) r J_1(pr)\, \mathrm{d}r, \quad \Phi_i(t, p, z) = \int_0^{\infty} w_i(t, r, z) r J_0(pr)\, \mathrm{d}r.$$

Let us determine the Hankel transforms of Eqs. (4) and (5), and the boundary and continuity conditions for thermal stresses and displacements u_i, w_i in the radial and axial directions, respectively:

$$(1 - 2\nu_i) \frac{\partial^2 \varphi_i}{\partial z^2} - p \frac{\partial \Phi_i}{\partial z} - 2(1 - \nu_i) p^2 \varphi_i = -2\alpha_i (1 + \nu_i) p \theta_i(t, p, z), \tag{15}$$

$$2(1 - \nu_i) \frac{\partial^2 \Phi_i}{\partial z^2} + p \frac{\partial \varphi_i}{\partial z} - (1 - 2\nu_i) p^2 \Phi_i = 2\alpha_i (1 + \nu_i) \frac{\partial \theta_i(t, p, z)}{\partial z}, \tag{16}$$

$$(\bar{\sigma}_{zz})_i = 2G_i\left[\frac{1-\nu_i}{1-2\nu_i}\left(\frac{\partial\Phi_i}{\partial z}+p\varphi_i\right)-p\varphi_i-\frac{1+\nu_i}{1-2\nu_i}\alpha_i\theta_i\right], \tag{17}$$

$$(\bar{\sigma}_{rz})_i = G_i\left(\frac{\partial\varphi_i}{\partial z}-p\Phi_i\right), \tag{18}$$

$$(\bar{\sigma}_{rz})_n=(\bar{\sigma}_{zz})_n=0 \text{ at } z=\Delta, \quad (\bar{\sigma}_{zz})_1^-=(\bar{\sigma}_{zz})_0 \text{ at } z=0,$$

$$(\bar{\sigma}_{rz})_{i-1}=(\bar{\sigma}_{rz})_i, \quad (\bar{\sigma}_{zz})_{i-1}=(\bar{\sigma}_{zz})_i, \quad \Phi_{i-1}=\Phi_i, \quad \varphi_{i-1}=\varphi_i. \tag{19}$$

After some algebra (for details, see [11]), Eqs. (15) and (16) can be rewritten as

$$\frac{\partial}{\partial z}\left(\frac{\partial\varphi_i}{\partial z}-p\Phi_i\right)-2\frac{\nu_i p}{1-2\nu_i}\left(\frac{\partial\Phi_i}{\partial z}+p\varphi_i\right)-2p^2\varphi_i = -2\alpha_i p\frac{1+\nu_i}{1-2\nu_i}\theta_i(t,p,z). \tag{20}$$

$$2\frac{\partial}{\partial z}\left[\frac{1-\nu_i}{1-2\nu_i}\left(\frac{\partial\Phi_i}{\partial z}+p\varphi_i\right)-p\varphi_i-\frac{1+\nu_i}{1-2\nu_i}\alpha_i\theta_i(t,p,z)\right] = -p\left(\frac{\partial\varphi_i}{\partial z}-p\Phi_i\right). \tag{21}$$

Equations (20) and (21), after substitution of Eq. (17), yield

$$\frac{\partial}{\partial z}(\bar{\sigma}_{rz})_i = \left(\frac{p}{1-\nu_i}\right)\left[\nu_i(\bar{\sigma}_{zz})_i+2G_i p\varphi_i-2(1+\nu_i)\alpha_i G_i\theta_i(t,p,z)\right]$$

$$\frac{\partial(\bar{\sigma}_{zz})_i}{\partial z} = -p(\bar{\sigma}_{rz})_i. \tag{22}$$

Integrating Eq. (22) over the thickness of the layer Δ_i, we obtain

$$(\bar{\sigma}_{rz})_i^+-(\bar{\sigma}_{rz})_i^- = \frac{p}{1-\nu_i}\int_{s_{i-1}}^{s_i}\left[\nu_i(\bar{\sigma}_{zz})_i+2pG_i\varphi_i(z) -2(1+\nu_i)\alpha_i G_i\theta_i(t,p,z)\right]\mathrm{d}z,$$

$$(\bar{\sigma}_{zz})_i^+-(\bar{\sigma}_{zz})_i^- = -p\int_{s_{i-1}}^{s_i}(\bar{\sigma}_{rz})_i\mathrm{d}z,$$

$$s_i=\sum_{j=0}^{i}\Delta_j, s_0=0, \quad i=1\ldots n. \tag{23}$$

Summing up Eq. (23) over all the layers in a coating (from $i=1$ to n) and, taking into account the boundary conditions of Eq. (18), we obtain

$$\bar{\sigma}_{rz}(0) = -\sum_{i=1}^{n} \frac{p}{1-\nu_i} \int_{s_{i-1}}^{s_i} \left[\nu_i (\bar{\sigma}_{zz})_i + 2pG_i\varphi_i(z) - 2(1+\nu_i)\alpha_i G_i \theta_i(t, p, z)\right] dz,$$

$$\bar{\sigma}_{zz}(0) = p \sum_{i=1}^{n} \int_{s_{i-1}}^{s_i} (\bar{\sigma}_{rz})_i dz. \tag{24}$$

Integrating Eq. (17) for $(\bar{\sigma}_{zz})_i$ over the thickness of a layer Δ_i and summing up the obtained expressions from $i=1$ to n, taking into account that $\Phi_{i-1}^{+} = \Phi_i^{-}$, yields

$$\Phi(z=\Delta) = \Phi(z=0) + \frac{1}{1-\nu_i} \sum_{i=1}^{n} \int_{s_{i-1}}^{s_i} \left[\frac{1-2\nu_i}{2G_i} (\bar{\sigma}_{zz})_i - \nu_i p\varphi_i(z) + (1+\nu_i)\alpha_i\theta_i\right] dz. \tag{25}$$

Let us estimate the order of magnitude of the stress tensor component $\bar{\sigma}_{zz}$ in Eqs. (24) and (25). Since according to Eq. (24) the stress $\bar{\sigma}_{zz}$ is of the order of $(p\Delta)\bar{\sigma}_{rz}$, the integral of $\bar{\sigma}_{zz}$ over z can be neglected. Calculation of the radial displacement $\varphi_i(z)$ using Eqs. (34) and (35) for a single-layer coating shows that for the case of a thin coating ($\Delta < 100\,\mu$m) the function φ_i varies weakly with coordinate z. Thus, e.g., the relative variation $(\varphi(\Delta) - \varphi(0))/\varphi(0)$ is equal to 0.017 and 0.023 for thicknesses of 50 and 90 μm, respectively. Therefore, in Eqs. (24) and (25), $\varphi_i(z)$ can be replaced by $\varphi_i(0)$;

$$\bar{\sigma}_{rz}(0) = -\frac{2p^2}{1-\nu}\varphi_1(0) \sum_{i=1}^{n} G_i\Delta_i + 2p\frac{1+\nu}{1-\nu} \sum_{i=1}^{n} \alpha_i G_i \int_{s_{i-1}}^{s_i} \theta_i(t, p, z)\, dz, \tag{26}$$

$$\Phi(\Delta) = \Phi_1(0) - \frac{\nu}{1-\nu}(p\Delta)\varphi_1(0) + \frac{1+\nu}{1-\nu} \sum_{i=1}^{n} \alpha_i \int_{s_{i-1}}^{s_i} \theta_i(t, p, z)\, dz. \tag{27}$$

We assume that $\nu_i = \nu$ because the magnitude of ν_i weakly influences the axial displacement w_n. In our previous study (see [7], Eq. (29)), we solved Eqs. (20) and (21) for a substrate ($i=0$) and determined the displacements $\Phi_1(0), \varphi_1(0)$, and the thermal stresses $\bar{\sigma}_{rz}(0), \bar{\sigma}_{zz}(0)$:

$$\bar{\sigma}_{rz}(0) = \frac{G_0}{4(1-\nu)} \left[N_0 - 4(1-\nu)D_0 - 4\alpha_0 p(1+\nu) \int_{-\infty}^{0} \theta_0(t, p, z)\cosh(pz)\, dz\right],$$

$$\bar{\sigma}_{zz}(0) = \frac{G_0}{4(1-\nu)} \left[N_0 + 4(1-\nu)D_0 - 4\alpha_0 p(1+\nu) \int_{-\infty}^{0} \theta_0(t, p, z)\sinh(pz)\, dz\right],$$

$$\Phi_1(0) = \frac{3-4\nu}{8p(1-\nu)}N_0 + \frac{1}{2}D_0 + \frac{1+\nu}{(1-\nu)}\alpha_0 p\int_{-\infty}^{0}\theta_0(t,p,z)\exp(pz)\,\mathrm{d}z,$$
$$\varphi_1(0) = \frac{3-4\nu}{8p(1-\nu)}N_0 - \frac{1}{2}D_0 + \frac{1+\nu}{(1-\nu)}\alpha_0 p\int_{-\infty}^{0}\theta_0(t,p,z)\exp(-pz)\,\mathrm{d}z, \qquad (28)$$

where D_0, N_0 are the integration constants. Taking into account that $\bar{\sigma}_{rz}$ is a continuous function of coordinate z and the thickness $\Delta/r_0 \ll 1$, Eq. (24) becomes

$$\bar{\sigma}_{zz}(0) = p\sum_{i=1}^{n}\int_{s_{i-1}}^{s_i}(\bar{\sigma}_{rz})_i\,\mathrm{d}z = (p\Delta)\,\bar{\sigma}_{rz}(0)\ . \qquad (29)$$

Substituting Eq. (28) into Eqs. (26), (27), and (29), after some algebra one can determine the integration constants D_0, N_0 and the axial surface displacement w_n:

$$w_n(r, z=\Delta) = \int_0^\infty \Phi(\Delta)\,pJ_0(pr)\,\mathrm{d}p$$
$$= \alpha_0\frac{1+\nu}{1-\nu}\int_0^\infty\left\{\frac{1+L_n}{1+p\Delta}\int_{-\infty}^{0}\exp(pz_0)\theta_0(p,z_0)\,\mathrm{d}z_0\right.$$
$$\left.+\sum_{i=1}^{n}\frac{\alpha_i}{\alpha_0}\left(L_n\frac{G_i}{G_0}+1\right)\int_{s_{i-1}}^{s_i}\theta_i(p,z)\,\mathrm{d}z\right\}pJ_0(pr)\,\mathrm{d}p. \qquad (30)$$

Here

$$L_n = \left(A_n - A_p\frac{\nu}{1-\nu}p\Delta\right)\left[\frac{2}{1+p\Delta}+\frac{1}{1-\nu}A_p p\sum_{i=1}^{n}\frac{G_i}{G_0}\Delta_i\right]^{-1},$$
$$A_p = 3-4\nu+(1-p\Delta)/(1+p\Delta), \quad A_n = 3-4\nu-(1-p\Delta)/(1+p\Delta).$$

This expression can be simplified, provided that $\Delta/r_0 \ll 1$:

$$L_n = 1-2\nu,$$
$$w_n = 2\alpha_0(1+\nu)\left\{\int_0^\infty\int_{-\infty}^{0}\exp(pz_0)\,\theta_0(p,z_0)\,pJ_0(pr)\mathrm{d}p\,\mathrm{d}z_0\right.$$
$$\left.+\frac{1}{2(1-\nu)}\sum_{i=1}^{n}\frac{\alpha_i}{\alpha_0}\left[1+(1-2\nu)\frac{G_i}{G_0}\right]\int_{s_{i-1}}^{s_i}T_i(z_0)\mathrm{d}z_0\right\}. \qquad (31)$$

The probe beam deflection angle is obtained by differentiating Eqs. (30) and (31) with respect to the radial coordinate:

$$\varepsilon(r,t) = 2\left|\frac{\partial w_n}{\partial r}\right|_{z=\Delta}. \qquad (32)$$

Equation (31) is obtained under the assumption that a coating is composed of n layers manufactured from different homogeneous materials. In order to extend this expression to an FGM material, whereby physical properties vary continuously with coordinate z, we consider the limiting case when $\Delta_i \to 0$ and $n \to \infty$. Replacing the summation over i by integration over coordinate z, we obtain

$$w(r,\Delta) = \frac{1+\nu}{1-\nu}\int_0^\infty \left\{ \alpha_0 \frac{1+L}{1+p\Delta}\int_{-\infty}^0 \exp(pz_0)\theta_0(p,z_0)\,\mathrm{d}z_0 + \int_0^\Delta \alpha(z)\left(L\frac{G(z)}{G_0}+1\right)\times\theta(p,z)\,\mathrm{d}z \right\} pJ_0(pr)\,\mathrm{d}p, \quad (33)$$

where

$$L = (1-2\nu)(1+2p\Delta)\left(1+2p\int_0^\Delta \frac{G(z)}{G_0}\mathrm{d}z\right)^{-1}.$$

3. SOLUTION OF THE PROBLEM FOR THE CASE OF A SINGLE-LAYER COATING

In this particular case, we obtained the exact analytical solution of the elasticity problem (Eqs. (4) and (6)) in order to compare it with the approximate solution (Eqs. (30) and (31), (n = 1)). Temperature distributions in a coating ($n=1$) and a substrate ($n=0$) are given by Eq. (14), provided that $Fo = k_0 t/d^2 \ll 1$. An analytical solution of Eqs. (15) and (16) was obtained in our previous study [7] and can be written in the following form:

$$F_i^{\pm} = \frac{1}{2}\left[C_i\exp(-pz) \pm D_i\exp(pz)\right] + \frac{M_i}{4(1-\nu_i)}\left[z \pm \frac{3-4\nu}{2p}\right]\exp(-pz) + \frac{N_i}{4(1-\nu_i)}\times\left[\mp z + \frac{3-4\nu}{2p}\right]\exp(pz) + \frac{\alpha_i}{2}\frac{1+\nu_i}{1-\nu_i}\int_{\bar{z}}^{z}\theta_i(t,p,z_0)\left\{\exp[p(z_0-z)] \pm \exp[-p(z_0-z)]\right\}dz_0, \quad (34)$$

where

$$\bar{z} = \begin{cases} -\infty, & i=0 \\ 0, & i=1 \end{cases},$$

C_i, D_i, M_i, N_i are integration constants ($M_0 = C_0 = 0$), $F_i^+ \equiv \Phi_i$, and $F_i^- \equiv \varphi_i$ ($i = 0, 1$). Substituting Eq. (34) into Eqs. (17) and (18) we find that

$$\bar{\sigma}_{irz} = G_i \left[M_i \exp(-pz) + N_i \exp(pz) - 2pF_i^+ \right],$$
$$\bar{\sigma}_{izz} = G_i \left[-M_i \exp(-pz) + N_i \exp(pz) - 2pF_i^- \right]. \tag{35}$$

Taking into account the continuity conditions in Eq. (19) and Eqs. (28), (34), and (35), we arrive at the system of algebraic equations for integration constants M_1 and N_1, which are used later for determining the axial displacement:

$$-2(p\Delta)M_1 + \left[\exp(2p\Delta) - 1 + \frac{4(1-\nu)}{1+\bar{G}(3-4\nu)} \right] N_1$$
$$= \frac{16\alpha_0 (1-\nu^2)\, p}{1+\bar{G}(3-4\nu)} \int_{-\infty}^{0} \theta_0(t, p, z_0) \exp(pz_0)\, dz_0 + 4\alpha_1 (1+\nu)\, p$$
$$\times \int_0^{\Delta} \theta_1(t, p, z_0) \exp(pz_0)\, dz_0,$$
$$\left[\exp(-2p\Delta) - 1 + \frac{4(1-\nu)}{1-\bar{G}} \right] M_1 + 2(p\Delta)N_1$$
$$= 4\alpha_1 (1+\nu)\, p \int_0^{\Delta} \theta_1(t, p, z_0) \exp(-pz_0)\, dz_0, \tag{36}$$

where $\bar{G} = G_1 / G_0$. We assumed that Poisson's ratios of a coating and a substrate are equal, i.e., $\nu_0 = \nu_1 = \nu$ because the magnitudes of ν_0, ν_1 weakly affect the displacement w_1. Taking into account Eqs. (34) and (35), the expression for an axial displacement w_1 of the coating surface ($z = \Delta$) can be written as

$$w_1(t, r) = \int_0^{\infty} \Phi_1(t, p, z = \Delta)\, p J_0(pr)\, dp$$
$$= \frac{1}{2} \int_0^{\infty} [M_1 \exp(-p\Delta) + N_1 \exp(p\Delta)] J_0(pr)\, dp. \tag{37}$$

For the particular case of a thin coating ($\Delta / r_0 \ll 1$), Eqs. (36) and (37) yield

$$w_1(t, r) = 2\alpha_0 (1+\nu) \int_{-\infty}^{0} \int_0^{\infty} \exp(pz_0)\, \theta_0(t, p, z_0)\, p J_0(pr)\, dp dz_0$$
$$+ \alpha_1 \frac{1+\nu}{1-\nu} \left[1 + \bar{G}(1-2\nu) \right] \int_0^{\Delta} T_1(t, r, z_0) dz_0. \tag{38}$$

The probe beam deflection angle ε is determined by the slope of an irradiated surface according to Eq. (32). Equation (38) is identical to Eq. (31)

($n = 1$) obtained by the approximate analytical procedure. We calculated the axial displacement w_1 from Eq. (36) in the range $10\,\mu\text{m} < \Delta < 100\,\mu\text{m}$ and found that the maximum deviation of the approximate Eq. (26) from the exact Eq. (37) does not exceed 2%.

We also obtained an analytical solution of the problem for a particular case when a coating is removed ($\Delta = 0, i = 0$) and the duration of a pump laser pulse $\tau_0 \ll t$. The inverse Laplace transform of Eq. (11) reads ($a_n = b_n = 1,\ \Delta_n = 0$)

$$\theta_0(t, p, z) = \frac{E_0}{2\pi^{3/2}} \frac{\sqrt{k_0}}{\lambda_0 \sqrt{t}} \exp\left\{ -\left[\frac{z^2}{4k_0 t} + p^2 \left(0.25 r_0^2 + k_0 t \right) \right] \right\}. \tag{39}$$

Substituting Eq. (39) into Eq. (38), one can obtain the following formulae for the axial displacement w_0 and the probe beam deflection angle ε_0 for the case of a specimen without a coating:

$$w_0(t, r) = \frac{E_0 \alpha_0 (1 + \nu)}{\pi c_0} \int_0^\infty \operatorname{erfc}\left(p\sqrt{k_0 t} \right) \exp\left(-0.25 p^2 r_0^2 \right) p J_0(pr)\, \mathrm{d}p. \tag{40}$$

$$\begin{aligned} \varepsilon_0(t, r) &= 2 \left| \frac{\partial w_0}{\partial r} \right|_{z=0} \\ &= \frac{2 E_0 \alpha_0 (1 + \nu)}{\pi c_0} \int_0^\infty \operatorname{erfc}\left(p\sqrt{k_0 t} \right) \exp\left(-0.25 p^2 r_0^2 \right) p^2 J_1(pr)\, \mathrm{d}p, \end{aligned} \tag{41}$$

where

$$\operatorname{erfc}(x) = \frac{2}{\sqrt{\pi}} \int_x^\infty \exp\left(-x^2 \right) \mathrm{d}x$$

4. RESULTS AND DISCUSSION

First, we compared the magnitudes of the surface displacement w and the beam deflection angle ε for the particular case of a single-layer coating obtained using approximate Eqs. (30) and (31) with the exact analytical solution of Eqs. (36) and (37). Calculations of w and ε were performed over a wide range of thicknesses $10 < \Delta < 100\,\mu\text{m}$ and in the time interval $10 < t < 500\,\mu\text{s}$. The relative difference of the results does not exceed 2% for the displacement w and 3% for the deflection angle ε. Therefore, the results obtained using Eqs. (30) and (37) are in fairly good agreement. In order to prevent a "mirage" effect [6] caused by heating of the air near the

coating surface (especially, for the case of a low thermal-diffusivity coating, see Ref. 1) it is necessary to perform the photothermal experiment in a chamber evacuated to a low pressure (in Ref. 1 the pressure of air over the heated surface was 2 Pa).

In order to determine the physical properties of the multilayered or functionally graded coating using the "thermal mirror" method, it is necessary to measure these properties after deposition of every individual thin layer ("layer by layer"), beginning with a first layer deposited on a substrate and ending with an external layer. Since the physical properties vary from layer to layer, also, the surface displacement w and the probe beam deflection angle ε change with an increase in the thickness of the coating. Therefore, by measuring the deflection angles ε_{n-1}, ε_n consequently, before and after deposition of a layer n, and, comparing the results of measurements with theoretical predictions, one can determine the physical properties of this layer. For this purpose, we determined the ratio $R_n = \varepsilon_n/\varepsilon_{n-1}$ from Eqs. (30) and (32):

$$\begin{aligned} R_n &= \frac{\varepsilon_n(t)}{\varepsilon_{n-1}(t)} \\ &= \frac{\alpha_n c_{n-1}}{\alpha_{n-1} c_n} \frac{1+(1-2\nu)(G_n/G_0)}{1+(1-2\nu)\left(G_{n-1}/G_0\right)} Z_n\left(k_n, k_{n-1}, t\right), \\ Z_n(t=0) &= 1. \end{aligned} \tag{42}$$

The function Z_n depends mainly on the rate of relaxation of the temperature field in a coating, i.e., on the thermal diffusivity k_n of the external layer and time t. Therefore, this function can be used for determining k_n. The ratio R_n determines the change in the deflection angle ε after deposition of the external layer n.

Consider the results obtained for a specimen composed of a substrate (Ni) and a single-layer coating with the following volume contents of ZrO_2 ceramics: Ni (60%) + ZrO_2 (40%) and Ni (20%) + ZrO_2 (80%). The operating parameters of a laser beam are as follows: $E_0 = 0.01$ J, $r_0 = 1$ mm, and the duration of a laser pulse $\tau_0 = 3\,\mu$s. These parameters are obtained from calculations of the temperature distribution (Eq. (14)) in a specimen and the maximum value of the slope of an irradiated surface (Eqs. (38) and (41)). They give a maximum temperature rise of a specimen of 10–100 K (depending on the thermal conductivity), and a slope of an irradiated surface of the order of 10^{-5} (for the specimen with and without a coating). This magnitude of the slope allows measurements by a commercially available device. Calculations showed that the maximum values of ε are attained at the radial coordinate $r/r_0 \sim 0.8$, and hence the optimal distance between the power beam and the probe beam axes is in the range of

$r/r_0 = 0.8$ to 1, i.e., $r \sim 1$ mm. Outside this interval, the magnitude of the deflection angle ε decreases sharply.

In order to determine the thermal and mechanical properties of a coating, we used the approximate effective properties as the volume average values (m: metal, c: ceramics), i.e.,

$$c = (c)_m V_m + (c)_c V_c, \qquad \lambda^{-1} = \lambda_m^{-1} V_m + \lambda_c^{-1} V_c,$$
$$G = G_m V_m + G_c V_c, \qquad \alpha = \alpha_m V_m + \alpha_c V_c. \tag{43}$$

The physical properties of a substrate and a layer obtained using the expressions in Eq. (43) are presented in Table I. Using Eq. (14), we determined the temperature distribution in a specimen heated by a power laser beam, the axial displacement w_1 of the coating surface $z = \Delta$, and also the probe beam deflection angle ε. Figure 2 shows the temperature distribution in a coating (solid lines) for different values of time t. Due to the low thermal conductivity of a coating, there is a significant temperature difference ΔT between the surfaces $z = \Delta$ and $z = 0$ (up to 70 K at a distance of 20 μm). For comparison, for the case of a coating with a thermal conductivity identical to that for a substrate, the difference ΔT is equal to 5 K (curve 4). Calculations showed that for a time $t < 1$ ms, the temperature field was localized within a coating. During this time the buckling of the specimen surface was caused mainly by non-uniform thermal expansion of the coating. Using Eqs. (32), (36), and (37), we determined the axial displacement w of an irradiated specimen surface and the probe beam deflection angle ε that is the principal measured parameter in the photothermal displacement method. Calculations showed that the presence of a coating strongly affects the axial displacement $w(t)$ and deflection angle $\varepsilon(t)$ (Fig. 3). We investigated the dependence of the deflection angle on the volume content V_c of ZrO_2 ceramics and the thickness Δ of a coating. It is found that the physical properties of a coating (they depend on V_c) significantly affect the angle $\varepsilon(t)$, especially at $t < 1$ ms (curves 1–4, Fig. 3). Therefore, the time interval $\tau_0 < t < 1$ ms is preferable for carrying out the photothermal experiment. The thickness of a coating also affects the deflection angle ε, especially at $t > 1$ ms.

Consider the results obtained for the specimen composed of the substrate (Ni) and the double layer coating ($n = 2$) with the following volume contents of a metal (Ni) and a ceramic (ZrO_2): internal layer (Ni (60%) + ZrO_2(40%)) and external layer (Ni (20%) + ZrO_2(80%)). Figure 4 shows the dependence of the functions $Z_1(k_1, t)$ and $Z_2(k_1, k_2, t)$ vs. time t for the single- and double-layer coatings, respectively. It is found that the functions Z_1 and Z_2 depend strongly on the thermal diffusivities k_1 and k_2, and this dependence is particularly pronounced for the

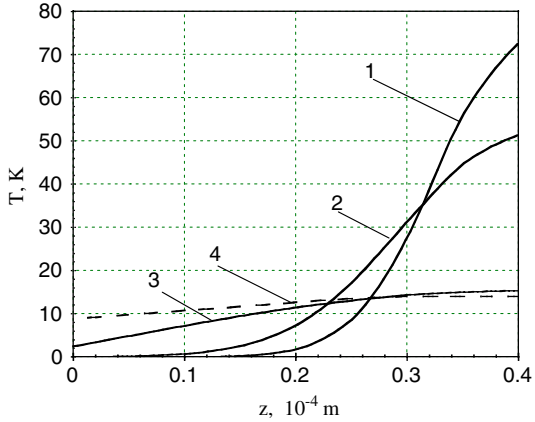

Fig. 2. Dependence of temperature T in a coating vs. axial coordinate z for different values of time t; curves: (1, 4) $t = 10^{-5}$ s, (2) $t = 10^{-4}$ s, (3) $t = 10^{-3}$ s.

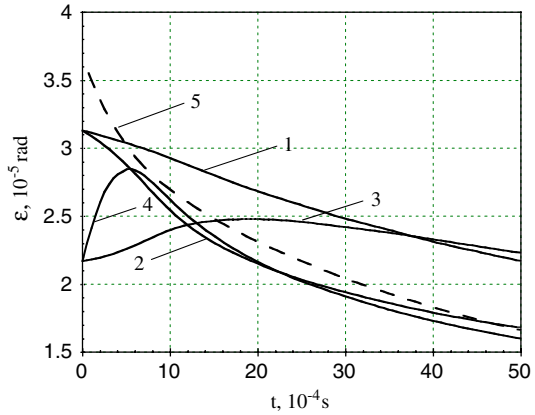

Fig. 3. Beam deflection angle $\varepsilon(r = 1\,\text{mm})$ vs. time t; curves: (1) $V_c = 40\%$, $\Delta = 40\,\mu$m; (2) $V_c = 40\%$, $\Delta = 10\,\mu$m; (3) $V_c = 80\%$, $\Delta = 4\,\mu$m; (4) $V_c = 80\%$, $\Delta = 1\,\mu$m; (5) without a coating.

case of a small thickness Δ_2 of the external layer (curve 6). We found that the photothermal displacement method is most sensitive when applied to a thin coating. Let us compare the function Z for the following two kinds of coatings: a single-layer ($Ni + ZrO_2(40\%)$) coating with a thickness of $\Delta_1 = 100\,\mu$m and a double-layer coating that is composed of the same internal layer and of the external thin layer ($\Delta_2 = 10\,\mu$m) with

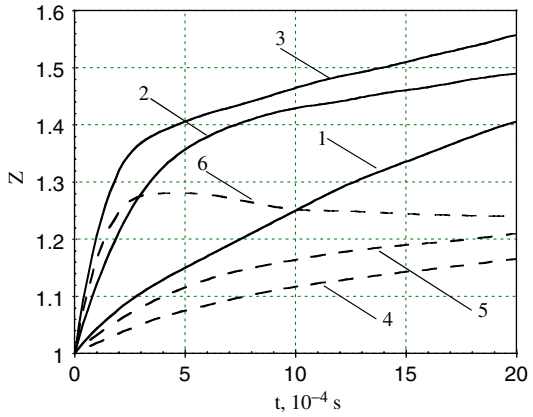

Fig. 4. Dependence of function Z vs. time t; curves: (1, 2, 3) single-layer coating, $\Delta_1 = 100$, 20, and 10 μm, respectively; (4, 5, 6) double-layer coating, $\Delta_1 = 100\,\mu$m, $\Delta_2 = 30$, 20, and 10 μm, respectively.

different volume content of ceramic ZrO_2(80%). Calculations showed that, although the thickness of the external layer was small, $\Delta_2 \ll \Delta_1$, the external layer strongly affects the beam deflection angle and, also, significantly changes the temporal dependence of the function Z in comparison with the single-layer coating (see Fig. 4, curves 1 and 6). This change is caused, mainly, by different values of the thermal diffusivities k_1 and k_2. Thus, one can determine k_2 comparing the measured values of R with the theoretical predictions given by Eqs. (30), (32), and (42).

Consider the effect of the volume content V_c of ceramic ZrO_2 in a coating on the beam deflection angle $\varepsilon(r = 1\,\text{mm})$ (see Fig. 5). For comparison, the dependence of ε with time t (curve 1) is given for a substrate without a coating. Curves 2 and 3 are obtained for a single-layer coating ($V_c = 40\%$), curves 4, 5—for a double-layer coating composed of the internal ($V_c = 40\%$) and external ($V_c = 80\%$) layers. Physical properties of the layers are presented in Table I. It is found that the volume content of ceramic V_c affects the beam deflection angle ε, especially for the case of a thin layer. Thus, e.g., the presence of a single-layer coating with a thickness of $\Delta_1 = 30\,\mu$m deposited on a substrate changes the angle ε by 40% (curves 1, 3, Fig. 5). A thin external layer ($V_c = 80\%$) in a double-layer coating decreases the angle ε and the surface displacement w in comparison with a single-layer coating (curves 3 and 5), especially for $t < 10^{-4}$ s. Therefore, the maximum sensitivity of the photothermal displacement method is achieved for the case of thin coatings. This property

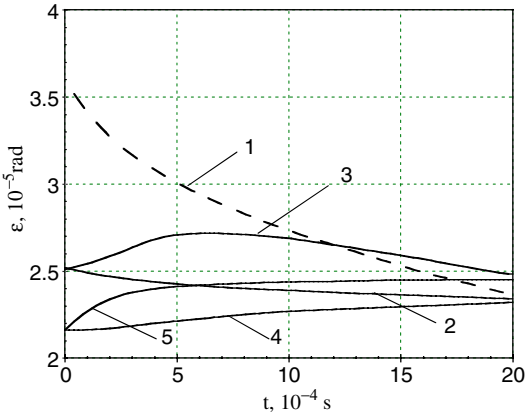

Fig. 5. Beam deflection angle $\varepsilon(r = 1\,\text{mm})$ vs. time t. Curves: (1) substrate without a coating; (2, 3) single-layer coating, $\Delta_1 = 100$ and $30\,\mu$m, respectively; (4, 5) double-layer coating, $\Delta_1 = 100\,\mu$m, $\Delta_2 = 30$ and $10\,\mu$m, respectively.

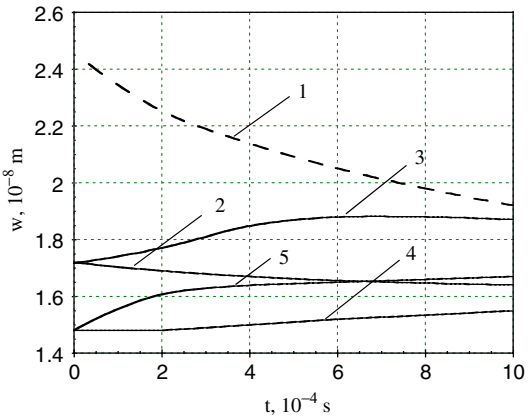

Fig. 6. Surface displacement $w(r = 0)$ vs. time t. Curves: (1) substrate without a coating; (2, 3) single-layer coating, $\Delta_1 = 100$ and 30μm, respectively; (4, 5) double-layer coating, $\Delta_1 = 100\,\mu$m, $\Delta_2 = 30$ and $10\,\mu$m, respectively.

is of great importance in application of the photothermal displacement method for measuring physical characteristics of functionally graded coatings (Fig. 6).

The procedure for determining the physical properties of a double-layer coating can be described as follows:

Stage 1: Measure the thermal diffusivity k_0 of a substrate (without a coating) by the photothermal method and compare with the results obtained previously by other experimental methods. This allows determination of the accuracy of the photothermal method and adjustment of the positioning of the power and probe laser beams. Taking into account that for small values of t,

$$\operatorname{erfc}\left(p\sqrt{k_0 t}\right) = 1 - \frac{2}{\sqrt{\pi}} p\sqrt{k_0 t},$$

Eq. (41) yields

$$\frac{\varepsilon_0(\tau_0) - \varepsilon_0(t)}{\varepsilon_0(\tau_0)} = \frac{2\sqrt{k_0 t}}{\sqrt{\pi} r_0} \frac{I_3}{I_2}, \tag{44}$$

where

$$I_n(r) = (r_0)^{n+1} \int_0^\infty \exp\left(-0.25 p^2 r_0^2\right) p^n J_1(pr)\, \mathrm{d}p.$$

In order to determine k_0, it is necessary to measure the probe beam deflection angle ε at two times, immediately after applying a power laser beam at a specimen, $\varepsilon_0(\tau_0)$, and after some time t, $\varepsilon_0(t)$, provided that $t \ll r_0^2/4k_0$. Substituting the experimental values of ε, radius r_0 of a power beam, time t, and the ratio I_3/I_2 (it depends only on the radial coordinate r) into Eq. (44), one can determine the thermal diffusivity k_0 of a substrate. It is important that the ratio in Eq. (44) does not depend on the total laser power E_0 absorbed by a specimen and, therefore, it does not influence the accuracy of determining k_0.

Stage 2: Determine two of the physical properties of a single-layer coating $(c_1, k_1, \alpha_1, G_1)$ provided that the remaining two properties are previously measured or calculated from Eq. (43). For this purpose, it is necessary to measure the dependence of the ratio $(\varepsilon_1/\varepsilon_0)_{\exp}$ vs. time t between the values of the deflection angle for a specimen with and without a coating. Equation (42) for small values of the time $t \ll \Delta^2/k_1$ yields

$$\frac{\varepsilon_1}{\varepsilon_0} = \frac{\alpha_1}{2\alpha_0} \frac{c_0}{c_1} \frac{1 + \bar{G}(1 - 2\nu)}{1 - \nu}, \tag{45}$$

where $\bar{G} = G_1/G_0$. The latter result is fairly insensitive to the value of ν for typical values of this parameter, i.e., $\nu_0 = \nu_1 = \nu$. Comparing the ratio $\varepsilon_1/\varepsilon_0$ calculated by Eq. (45) with the experimental value $(\varepsilon_1/\varepsilon_0)_{\exp}$, one can determine one of the physical properties of a coating, e.g., the specific

heat c_1. The dependence of the ratio $(\varepsilon_1/\varepsilon_0)_{\exp}$ on time t is caused by heat transfer from the irradiated surface $z=\Delta$ into a coating and a substrate. Therefore, this ratio depends on the thermal diffusivity of a coating k_1 and of a substrate k_0 that was determined during the first stage of the experimental procedure. Thus, one can determine k_1 (and, also, $\lambda_1 = c_1 k_1$) comparing the measured magnitude $(\varepsilon_1/\varepsilon_0)_{\exp}$ with the predicted value from Eq. (45). We assumed that the absorbed energy E_0 is identical for the specimen with and without a coating. In order to enforce this condition, one can attach a thin metallic foil (with a high thermal conductivity) to the specimen surface irradiated by a power beam.

Stage 3: Determine two of the following four properties of the external layer $n=2$ of a coating, α_2, c_2, k_2, or G_2, provided that the remaining two properties are calculated using Eq. (43) or otherwise are known. For this purpose, it is necessary to measure the ratio $\varepsilon_2/\varepsilon_1$ (ε_1 and ε_2 are the probe beam deflection angles for the single- and double-layer coatings, respectively) as a function of time provided that $Fo = \left(k_2/\Delta_2^2 + k_1/\Delta_1^2\right) t < 1$. Equation (42) at the time $\tau_0 < t \ll \Delta_2^2/k_2$ (relaxation of a temperature field during this time interval does not occur, therefore, the function $Z_2 = 1$) for $n=2$ yields

$$R_2 = \left.\frac{\varepsilon_2}{\varepsilon_1}\right|_{t=0} = \frac{\alpha_2 c_1}{\alpha_1 c_2} \frac{1 + (1-2\nu)\,(G_2/G_0)}{1 + (1-2\nu)\,(G_1/G_0)}. \tag{46}$$

Comparing the ratio $\varepsilon_2/\varepsilon_1$ calculated by Eq. (46) with the experimental value $\left(\varepsilon_2/\varepsilon_1\right)_{\exp}$ one can determine one of the physical properties of a coating, e.g., the specific heat c_2. By measuring the dependence of the ratio $\left(\varepsilon_2/\varepsilon_1\right)_{\exp}$ vs. time t and comparing it with the predicted value from Eq. (42), one can determine k_2. Using Eqs. (30), (32), and (42), we estimated the sensitivity of the method to a variation in thickness and changes in physical properties for a two-layer coating–substrate assembly. The parameters of the assembly are as follows: $\Delta_1 = 100\,\mu\text{m}$, $V_1 = 40\%$, $\Delta_2 = 30\,\mu\text{m}$, $V_2 = 80\%$. We varied (within 20%) properties of the external coating layer, i.e., thickness Δ_2, thermal diffusivity k_2, shear module G_2, and coefficient of linear thermal expansion α_2. It is found that the beam deflection angle ε_2 varies by 1.5%, 20%, 2%, and 10% (for $t = 10^{-3}$s) with Δ_2, k_2, G_2, and α_2, respectively. For a time $t < 10^{-4}$ s, the angle ε_2 varies 20% with α_2. Therefore, the method is most sensitive to a variation of thermal diffusivity and coefficient of linear thermal expansion.

The suggested procedure ("layer by layer") can be performed also for coatings with an arbitrary number of layers.

5. CONCLUSION

We proposed an algorithm of the photothermal displacement ("thermal mirror") method for measuring physical properties of multilayer and functionally graded coatings deposited on a metal substrate. For this purpose, a specimen is irradiated by a focused laser beam resulting in buckling of an illuminated surface due to non-uniform thermal expansion. The probe beam of another laser, which monitors the slope of the sample surface is reflected from it at an angle depending on time and properties of the coating and substrate. The reflected probe beam is registered by a sensitive detector. Due to variations in the deflection angle ε with time, the axis of a probe beam is shifted with respect to the detector at a distance that is directly proportional to ε. We solved analytically the two-dimensional thermal elasticity problem, and determined the expressions for the photoinduced displacement and the slope of the coating surface as a function of time and the physical properties of a sample. It is found that the "thermal mirror" method is particularly sensitive for the case of thin coatings with a thickness of the order of 10–30 μm. Therefore, this method can be employed for measuring physical properties of thin multilayer coatings after deposition of each individual thin layer ("layer by layer"), beginning with a first layer deposited on a substrate and ending with an external layer.

NOMENCLATURE

c	specific heat
d	substrate thickness
E_0	total laser power absorbed by a specimen
F_0	Fourier number
G	shear module
I_0	laser beam intensity absorbed by a coating
$J_i\,(x)$	ith order Bessel function of the first kind
k	thermal diffusivity
r	radial coordinate
r_0	radius of a laser beam
p, s	parameters of Hankel (p) and Laplace (s) transforms with respect to r and t, respectively
t	time
T	temperature
$\overline{\theta}(s, p, z)$	Laplace–Hankel transform of temperature
u, w	radial and axial components of displacement
$V_\mathrm{m}, V_\mathrm{c}$	volume content (m: metal, c: ceramics)
z	axial coordinate

α	coefficient of linear thermal expansion
Δ	coating thickness
ε	laser beam deflection angle
λ	thermal conductivity
θ	Hankel transform of temperature
ν	Poisson's ratio
σ_{ij}	thermal stress
$\sigma_{\mathrm{rr}}, \sigma_{\Psi\Psi}$	radial and tangential stresses, respectively
τ_0	duration of a laser pulse

Subscripts

0	substrate
$i = 1, \ldots, n$	number of a layer in a coating

Superscript

$+, -$	upper and lower surfaces of a layer in a coating, respectively

REFERENCES

1. M. Olmstead, N. Amer, S. Kohn, D. Fournier, and A. Boccara, *J. Appl. Phys. A* **32**:141 (1983).
2. D. P. Almond and P. M. Patel, *Photothermal Science and Techniques* (Chapman and Hall, London, 1996), pp. 87–91, 120–134.
3. C. D. Martinsons, A. P. Levick, and G. J. Edwards, *Int. J. Thermophys.* **24:**1171 (2003).
4. J. Balderas-Lopez and A. Mandelis, *Rev. Sci. Instrum.* **74:**5219 (2003).
5. J. G. Bai, Z. Z. Zhang, G. Q. Lu, and D. P. H. Hasselman, *Int. J. Thermophys.* **26:**1607 (2005).
6. H. Machlab, W. A. McGahan, J. A. Woollam, and K. Cole, *Thin Solid Films* **224**:22 (1993).
7. T. Elperin and G. Rudin, *ASME J. Electron. Packag.* **120**:82 (1998).
8. Y. Nagasaka, T. Sato, and T. Ushiku, *Meas. Sci. Technol.* **12**:2081 (2001).
9. A. Neubrand, H. Becker, and T. Tschudi, *J. Mater. Sci.* **38**:4193 (2003).
10. N. Noda, R. Hetnarski, and Y. Tanigawa, *Thermal Stresses* (Lastran, New York, 2000), pp. 131–133.
11. T. Elperin and G. Rudin, *Heat Mass Transfer* **38**:625 (2002).